ELSEVIER

Polymer 41 (2000) 3759–3777

polymer

Kinetics of pressure-induced phase separation (PIPS) in polystyrene + methylcyclohexane solutions at high pressure

Y. Xiong[1], E. Kiran*

Department of Chemical Engineering, University of Maine, Orono, ME 04469-5737, USA

Received 21 January 1998; received in revised form 2 August 1999; accepted 6 August 1999

Abstract

Kinetics of pressure-induced phase separation in polystyrene + methylcyclohexane solutions at high pressures (up to 25 MPa) have been studied as a function of polymer molecular weight (50 000 and 700 000), polymer concentration (in the range from 4 to 16% by mass) and the quench depth (in the range of 0.1–2 MPa), using time- and angle-resolved light scattering in a unique high-pressure cell with a path length of 250 μm.

The results show that phase separation in solutions at critical polymer concentrations proceeds by spinodal decomposition which is displayed by a spinodal ring or a maximum in the scattered light intensities with angle. The time interval for the observation of spinodal ring was observed to depend on the quench depth. The ring collapse was observed to take place within the range of 3–160 s, shorter times being associated with deeper quenches. Phase separation in solutions at off-critical concentrations was observed to proceeded by nucleation and growth mechanism for shallow quenches (as reflected by the absence of a maximum in the angular variation of the scattered light intensities), but by the spinodal decomposition process for deep quenches.

The characteristic wave number q_m corresponding to the maximum scattered light intensity I_m was observed to be non-stationary and moved to lower wave numbers with time for all quenches leading to spinodal decomposition. The time evolution of q_m and I_m were observed to obey the power law approximations $q_m \sim t^{-\alpha}$ and $I_m \sim t^{\beta}$. The exponents α and β were found to increase with the quench depth, while however, maintaining a $\beta \cong 2\alpha$ relationship. The scaling characteristics of the structure factor were also analyzed. It was found that for a given quench depth the data at different times could be reduced to a single master curve when normalized with respect to the maximum in the scattered light intensity and the corresponding wave number. Calculations of the apparent diffusivity, based on the estimated values for the early stage characteristic wave number q_{m0}, gave values around 10^{-9} cm^2/s.

Keywords: Kinetics of phase separation; Pressure-induced phase separation; Polystyrene

1. Introduction

Kinetics of phase separation deals with the non-equilibrium relaxation processes following the transfer or quench of any material from a thermodynamically stable state into a thermodynamically unstable state. After quench, the system that is in a non-equilibrium state gradually evolves to an equilibrium state which consists of two or more coexisting phases. This process may proceed through a variety of mechanisms such as nucleation, spinodal decomposition, domain growth and coarsening. These mechanistic processes in phase separation are quite general and similarities have been found in a large class of materials such as inorganic glasses, metal alloys, fluid mixtures, and polymer blends and solutions [1]. Our interest is in understanding the phase separation processes in polymer solutions at high pressures.

Phase separation in polymer solutions is an integral step in polymer formation, processing and property modifications, which may be induced by a change in temperature, pressure or solvent composition. Many of the earlier studies on the kinetics of phase separation have been limited to systems at atmospheric pressures, and temperature quench has been almost exclusively used to induce phase separation. With the rapid developments in supercritical fluid-based processing in recent years, there is now a growing interest in understanding and documenting the influence of pressure on phase separation processes in polymer solutions [2]. This is because in these processes pressure is used as a key tuning parameter to regulate the solvent properties, and induce miscibility or phase separation. At present, studies that are specifically focused on the kinetics of phase

* Corresponding author. Tel.: +1-207-581-2286; fax: +1-207-581-2323.
E-mail address: Kiran@maine.edu (E. Kiran).
[1] Present address: Tempra Technology, Bradenton, FL 34203, USA.

0032-3861/00/$ - see front matter
PII: S0032-3861(99)00592-3

separation in polymer solutions are not only relatively few [3–9] but those that are conducted at high pressures are particularly rare [2,10–20], many of which are contributions from our laboratory.

The earliest work on polymer solutions can be traced back to van Aartsen and Smolders [3]. They studied temperature-induced spinodal decomposition in poly(2, 6-dimethyl-1, 4-phenyleneether) + caprolactam mixtures. For theoretical analyses, Van Aartsen [21] also incorporated the Flory–Huggins free energy into the Cahn–Hilliard type framework [22–26]. They studied the kinetics of phase separation by measuring the turbidity change after quench but no angle-dependent scattered light measurements were conducted, so the evolution of the structure factor could not be documented.

Besides this very early work, only a few other studies for "polymer + solvent" systems are reported in the literature. Kuwahara et al. [4,5] investigated the spinodal decomposition in the poly(dimethylsiloxane) + diethyl carbonate solutions. In their initial work, they measured the scattered light intensities at six angles up to 2.5° [4]. Later Kubota and Kuwahara reexamined the same polymer solution using an improved experimental system [5]. This new system employed a photodiode array with 512 pixels as the detecting sensor and could monitor the small angle region with high angular resolution. The important characteristics of this system are that both the refractive index and the density of the solvent and polymer are almost identical so that the effects of multiple scattering and sedimentation are almost eliminated. They were the first who demonstrated the Cahn–Hilliard exponential-law growth in polymer solutions and found that the linearized Cahn–Hilliard theory, which predicts a time invariant q_m (wavenumber of the dominant concentration fluctuation), is valid in the early stage of phase separation. They also found that, in addition to the main (most dominant) peak, a second peak in the higher-scattering-angle region in the spectrum is observed some time after the quench. They analyzed the scaling behavior in the later stages of phase separation and found that both peaks can be scaled into a universal master curve.

Another system that has been examined in detail is the polystyrene + cyclohexane solution. Lal and Bansil [6] conducted comparative experiments at the critical polymer concentrations for different molecular weight samples. The observation times were in the range from about 45 to 600 s. Analyses based on Cahn–Hilliard linear theory was performed for the initial stage ($t < 100$ s) of phase separation process. Even though, no stationary peak was observed, they found that the linear theory is still reasonable to characterize the early stage phase separation. They used the power law approximation to characterize the growth of the domain size. They found that the hydrodynamics might be more important in the earlier time of the phase separation than the late stage that is contradictory to the common perceptions. Scaling behavior of the structure factor at late stages were also examined in their study and certain discrepancies with Furukawa scaling function [27] were pointed out.

A series of interesting work has been conducted by Tanaka [7,8] for polystyrene + diethylmalonate solutions. He found that due to the dynamic asymmetry between the polymer long chains and the small molecule, critical dynamics and the phase separation kinetics are greatly affected by the polymer viscoelasticity. The argument is that the phase separation may no longer be diffusion-controlled as the order parameter is not necessarily the slowest variable as commonly assumed. This means, when great asymmetry is present for the components of the system, the collision time (contact time) of droplets may be less than the chain internal relaxation time. This makes the stress field strongly coupled with the concentration field and the coarsening mechanism is dominated by the viscoelastic effect. Tanaka further suggests that, if in fact these experimental observations are confirmed, there may be another dynamic universality class for the highly asymmetric systems such as polymer solutions that have been assumed to belong to the same dynamic universality class as classical fluids.

More recently, a time-resolved small-angle X-ray scattering study was carried out by Xie et al. [9] for semidilute polystyrene + dioctylphthalate solutions. These solutions were selected for their high viscosity and hence slower kinetics and longer time scale to facilitate the experimental observation. They found that linear theories were valid at short times and the exponential relaxation rate $R(q)$ of the structure factor was linear in q^2 in the low wavenumber region, which is in agreement with the mean-field theory for spinodal decomposition. Their analysis further suggested that entanglement effects might play a role during the phase separation in polymer solutions.

These studies discussed above were all conducted at near atmospheric conditions and the phase separations were almost exclusively induced by a temperature quench except in the study by Kuwahara et al. [5], where pressure quench was employed.

Compared to the temperature or solvent-induced phase separation methods, pressure quench has the advantage in that fast quench rates can be achieved uniformly within the sample. This method was pioneered by Wong and Knobler [28] in a study of the spinodal decomposition in "isobutyric acid + water" system. In their studies, the system is first equilibrated at a slightly elevated pressure above ambient condition, then upon introducing a small and fast pressure reduction (less than 0.2 MPa), a very shallow "effective" temperature quench is achieved. A recent example of this type of approach is the study on "3-methylpentane + nitroethane" system reported by Bailey and Cannell [29].

The studies on the kinetics of phase separation at high pressures are rare due to the difficult experimental conditions. Schneider and his co-workers examined phase separation kinetics in several small molecular systems [30–33] for liquid–liquid and liquid–gas phase separation. Among these fluid mixtures, "2-butoxyethanol + water" has been

one of the most extensively studied systems. In their study, a pressure-quench from 14 to 0.1 MPa could be achieved within about 0.1 ms by a rupture diaphragm. However, only transmitted light and scattered light intensities at 90° were recorded. They observed that, after the quench, the scattered light intensity goes through a maximum as a function of time, and the elapsed time for this maximum to appear is related to the quench depth. The same system was re-investigated recently by Sieber and Woermann [34] and Wells et al. [35]. The work by Sieber and Woermann focused in the vicinity of the critical point and examined the behavior of relaxation time of critical opalescence. In their approach, pressure quench was obtained by bursting a capillary glass tube. The characteristic time of such quenches is about 0.15 ms. Wells et al. [35] conducted experiments at pressures up to 20 MPa for different compositions using the Pressure Pulse Induced Critical Scattering (PPICS) technique. This technique originates from the Pulse Induced Critical Scattering (PICS) method initially developed by Derham et al. [36] in which the polymer solutions were subjected to a series of temperature pulses across the phase boundary for the spinodal determination. Instead of using a temperature pulse, Kiepen and Borchard [12] later adapted pressure as the control variable to induce phase separation (PPICS). This approach has been used in several recent studies for polymer solutions [13–16]. All quenches in these studies are typically conducted in the one-phase region, and the information about the non-equilibrium state, such as the location of spinodal, are inferred by extrapolation procedures established by Debye [37–39]. The scattered light intensities were monitored at a limited number of discrete angles.

Recently a new technique has been developed. In this technique known as MRPD [17], multiple rapid pressure drops are conducted to different depths of penetration into the metastable or unstable regions, and new phase formation and growth is followed by monitoring the transmitted and scattered light intensities at different angles. The technique utilizes two high-pressure cells to achieve the rapid pressure quench of different depths. The larger cell is a variable-volume cell equipped with a movable piston. It is used as the polymer loading and mixing chamber. The second cell, which is much smaller in volume, is used as scattering cell. The cells are initially brought to the same pressure and the system contents are fully circulated for polymer dissolution. After the complete dissolution of the polymer, the two cells are isolated from each other by closing the valves in between. The pressure in the large cell is then lowered by moving the piston to enlarge its internal volume to create a pressure difference between the scattering cell. The pressure-quench in the scattering cell, and thus phase separation, is then achieved by rapid opening of the isolation valve (which is air-actuated) between the scattering cell and the large cell. The quench rate can reach 1000 MPa/s and the quenches are easily reproducible which is very useful in comparative studies. The transmitted and scattered light intensities at selected angles are monitored. The time evolution and time-scale of phase separation as a function of the quench depth using this technique have been investigated for solutions of polystyrene and polyethylene in *n*-pentane [17–20].

Kojima et al. [40] recently reported an experimental apparatus for both time- and angle- resolved light scattering measurements at pressure up to 34.3 MPa and temperature up to 573 K. The capability of their system was demonstrated by the preliminary results on the polypropylene + trichlorofluoromethane solution. However, no detailed results by this apparatus have been reported yet.

We have recently developed a new system that is based on the MRPD technique with improved design to give greater versatility in the kinetic experiments [41]. The system is suitable to conduct both shallow and deep pressure quenches, and permits simultaneous measurements of the transmitted light intensity and the scattered light intensities over a continuous angle range up to 15°.

In the present paper, we present detailed experimental results on the kinetics of Pressure Induced Phase Separation (PIPS) in the polystyrene + methylcyclohexane system obtained with this new experimental system. Phase separation for these solutions have been investigated as a function of polymer concentration, polymer molecular weight, solution temperature and pressure, and quench depth. In most of the conventional experiments for spinodal decomposition in fluid systems, the quench depth in terms of equivalent temperature drop is often several or tens of mK. Such extremely shallow quenches can take advantage of the critical slowing down [42] and therefore enhance the temporal resolution of the observations and make the detailed theoretical study possible. This is however not the focus of present study. We are more interested in providing a general picture of PIPS at high pressures in order to guide practical applications. Therefore, both shallow and relatively deep quenches (ΔP up to 2.0 MPa or equivalently hundreds of mK in ΔT) have been explored in the current investigation. Despite their limitations, conventional analyses based on available theoretical models have also been carried out using the present experimental data.

2. Experimental section

2.1. Materials

Polystyrene (PS) samples of low polydispersity ($M_w = 700\,000$ with $M_w/M_n < 1.26$, and $M_w = 50\,000$ with $M_w/M_n < 1.06$) were obtained from Pressure Chemical Co.. Spectrophotometric grade (purity >99%) methylcyclohexane (MCH) was obtained from Aldrich.

2.2. Apparatus

Fig. 1 is a general layout of the experimental system. Full details of this unique system have been described in a

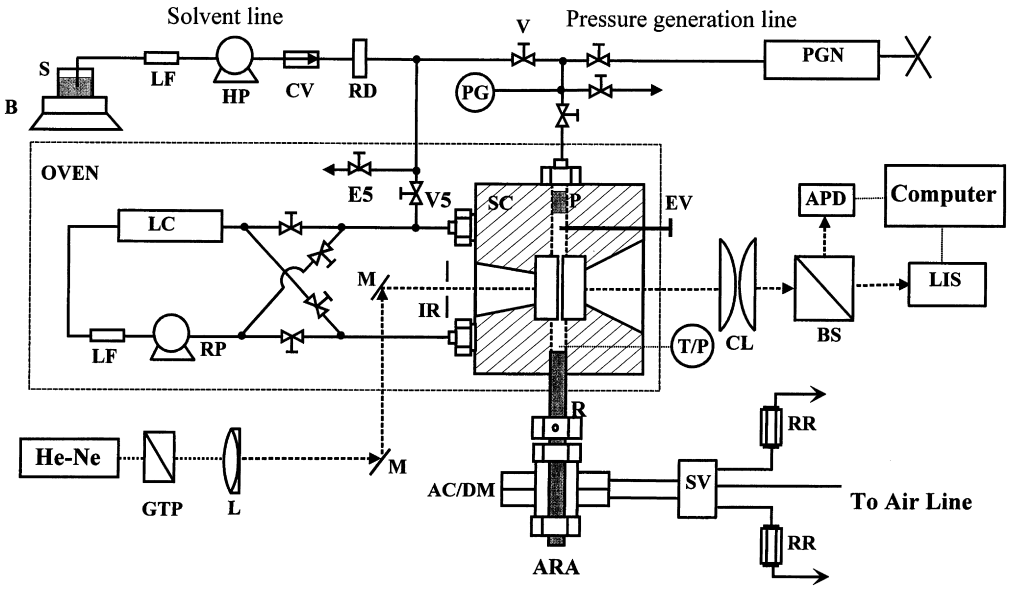

Fig. 1. General layout of the high-pressure high-temperature time- and angle-resolved light scattering system. (AC/DM, air cylinder/diaphragm; ARA, air-actuated rod assembly; APD, avalanche photodiode; B, balance; BS, beam splitter; CL, condensing lens; CV, check valve; EV, expansion valve; GTP, Glan-Thompson polarizer; HP, high pressure pump; IR, iris; L, focusing lens; LF, line filter; LIS, linear image sensor; M, mirror; LC, loading chamber; P, piston; PG, pressure gauge; PGN, pressure generator; R, movable rod; RR, release regulator; RD, rupture disk; RP, recirculation pump; S, solvent; SC, scattering cell; SV, solenoid valve; T/P, thermocouple/pressure transducer; V, V5, E5, valves; W, sapphire window).

previous publication [41]. Briefly, it consists of a solvent delivery line, a pressure generation line, a re-circulation pump (RP), a polymer loading and dissolution chamber (LC), a high-pressure variable-volume scattering cell (SC) (incorporating both a movable piston and an air-actuated rod assembly), and an optical system. The data acquisition and temperature and pressure controls are computerized. The scattering cell uses two flat sapphire windows (25.4 mm in diameter and 12.7 mm in thickness) separated with a very thin stainless-steel spacer that in the present cell leads to a path length of 250 μm. The cell is equipped with a built-in movable piston (P) connected to a pressure generator (PGN). By manipulating the pressure generator to change the position of the piston, the internal volume, and in turn, the pressure in the scattering cell can be changed. For very fast and deep pressure quenches, the air-actuated expansion rod assembly (ARA) installed at the bottom of the scattering cell is used. The rod is driven by high-pressure air cylinder upon a trigger signal from the computer, and rapidly changes the internal volume of the cell, leading to very fast pressure drops. The shallower quenches are achieved with the movement of a built-in valve stem (EV, expansion valve) in the cell cavity. The overall system is designed and has been tested at pressures up to 70 MPa and temperature up to 473 K with the control accuracy of ±0.02 MPa and ±0.05 K, respectively. For the optical unit, a He–Ne laser with wavelength of 632.8 nm passes through a Glan–Thompson polarizer (GTP) and is guided to the center of the scattering cell. On the exit side of the laser, two convex lenses (CL) are placed back to back to collect and transfer the scattering image to a linear image sensor (LIS). A beam splitter (BS), placed after the condensing lenses, sends the transmitted light to an Avalanche photo diode detector (APD). The linear image sensor has 256 pixels giving a continuous angular coverage of 1.9–12.7° in air for the present setup. The maximum sustainable data acquisition speed of the sensor is 3.2 ms/scan. Special data acquisition system allows continuous sampling at this maximum speed up to several minutes. A given phase separation process is thus followed by monitoring the time evolution of scattered light intensities for all angles in the range from 1.9 to 12.7°.

2.3. Procedure for determination of the demixing pressures

Prior to pressure-quench experiments, the demixing pressure for a given solution is determined as a reference point to establish the quench depth. The polymer is placed into the loading chamber LC (a high-pressure micro-reactor). Then the solvent is charged to the pre-vacuumed system, and the valve V5 is closed. The system is then pressurized at a given temperature by moving the piston in the top part of the scattering cell with the aid of the pressure generator. A gear pump is used to re-circulate the contents in the system to achieve dissolution. A set of properly configured valves is utilized to switch the flow direction to avoid any stagnant zones in the loop or in the scattering cell. In determination of the demixing pressures, after full homogenization of the polymer solution, the pressure is slowly decreased by moving the piston backwards (by reducing the pressure in the pressure generator) until the two-phase region is entered. The changes in the pressure and the transmitted light intensity as well as the temperature with time are recorded

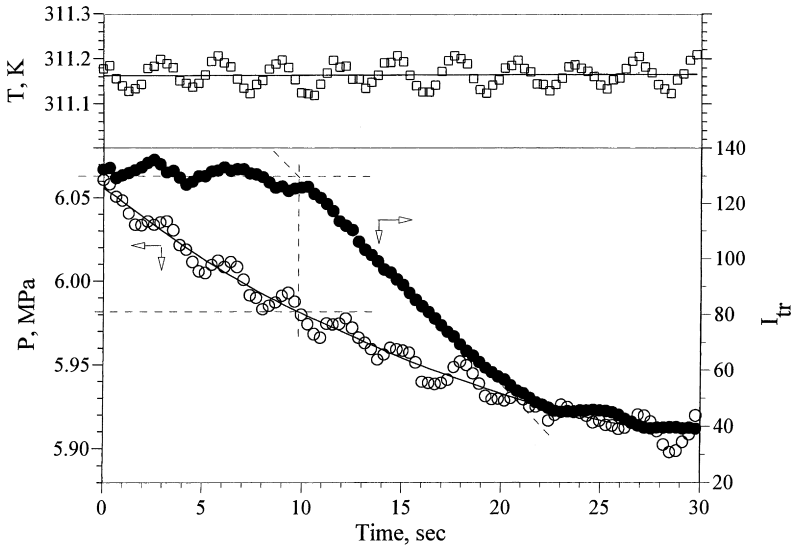

Fig. 2. Temperature, pressure and transmitted light intensity profiles during a slow pressure reduction to determine the demixing pressure for 4.6% by mass polystyrene ($M_w = 50\,000$) in methylcyclohexane. The turning point in the transmitted light intensity is taken as the incipient phase separation (demixing) point.

during the process. Fig. 2 shows, as an example, the changes in pressure, temperature and the transmitted light intensity during pressure reduction in 4.6% solution of polystyrene ($M_w = 50\,000$) in methylcyclohexane. After the system crosses the phase boundary, the transmitted light intensity start to decrease significantly. We record the pressure corresponding to this turning point in the transmitted light intensity as the demixing pressure. By repeating this procedure at different temperatures, the complete demixing P–T curves are generated for a given solution. It should be noted that the temperature remains very stable during these measurements that are conducted at a very slow rate (0.05 MPa/s) of pressure reduction.

2.4. Procedure for pressure-quench experiments

Once the demixing pressures are determined for a particular polymer solution, the solution is re-homogenized. Then, at a given temperature, the pressure of the system is carefully brought to about 0.1 MPa above the demixing pressure. When the temperature and pressure is equilibrated, the system is then subjected to the desired pressure-quench experiment. In the present study, majority of quenches were brought about by the movement of the expansion valve (EV, Fig. 1).

As an example, Fig. 3 shows the change in temperature, pressure and transmitted light intensity during a quench for

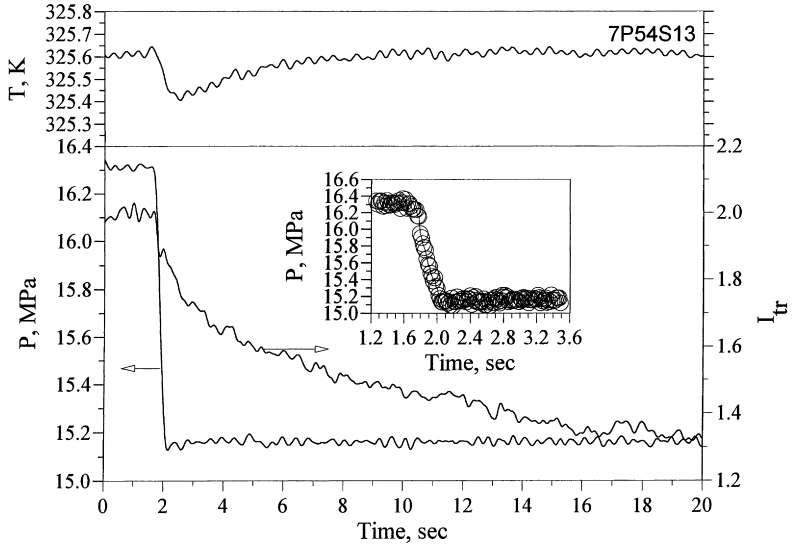

Fig. 3. Temperature, pressure and transmitted light intensity profiles during a relatively deep quench for 5.5% by mass polystyrene ($M_w = 700\,000$) in methylcyclohexane. The quench depth $\Delta P = 1.20$ MPa. The inset diagram shows the details of the transient change in pressure.

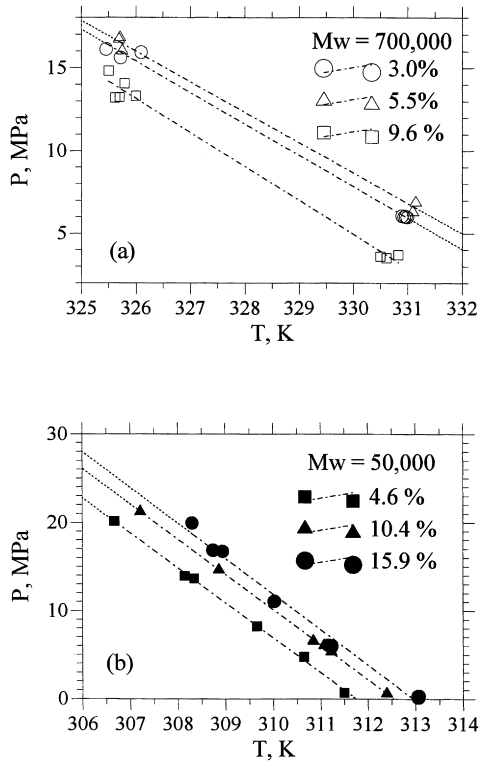

Fig. 4. The demixing (P–T) curves for polystyrene/methylcyclohexane at selected concentrations. Various lines are linear fits for better visualization. (a) $M_w = 50\,000$; (b) $M_w = 700\,000$.

a 5.5% solution ($M_w = 700\,000$) at 325.6 K with the movement of the expansion valve. Here a quench depth ΔP of 1.20 MPa has been achieved over 300 ms corresponding to a quench rate of about 4 MPa/s. It should be noted that the transmitted light intensity undergoes a significant reduction after phase separation. The temperature profile shows a quick drop immediately after the pressure quench and then rises back to its original value with time. The initial drop is due to Joule–Thompson effect of the nearly adiabatic quench, and the subsequent rise is a result of the heat flow from the metal enclosure and/or sapphire window to the sample solutions since their temperature remains essentially unchanged after the quench. It takes about 5 s for the temperature to rise back to its initial value. For shallower quenches, the time for temperature to return to its initial value is much shorter (about 2 s) [41].

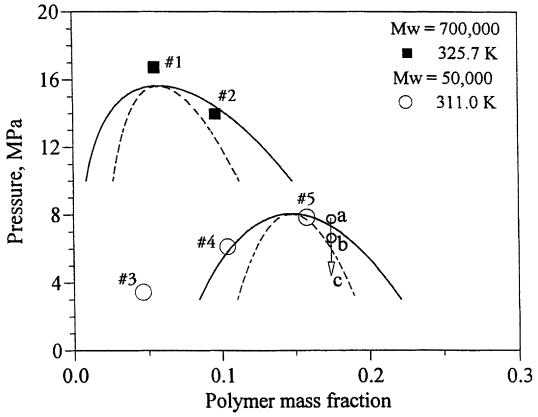

Fig. 5. The demixing (P–X) curves for polystyrene ($M_w = 50\,000$ and 700 000)/methylcyclohexane at selected temperatures. Solid and dashed curves are binodal and spinodal predicted by mean filed lattice gas model. Symbols represent experimental data points for the binodal and the spinodal points for solutions #1, 2, 4 and 5, which differ by less then 0.5 MPa. For solution #3, the symbol represents the binodal—spinodal for this solution could not be reached by the quench depths explored demonstrating the divergence of the spinodal curve from the binodal as one moves away from the critical polymer concentration.

2.5. Procedure for correction of the scattered light intensity

During each quench, in addition to changes in pressure, temperature, and transmitted light intensity, changes in the scattered light intensities are also monitored. The scattered light intensities are corrected for turbidity and background scattering prior to further interpretations of time evolution of new phase formation and growth.

By following the reasoning of Kiepen and Borchard [10–12], the raw data for the scattered light intensity can be corrected first to compensate for the turbidity according to

$$I_{s,\theta}^{corr} = I_{s,\theta}^{raw}/I_{tr}^{raw} \quad (1)$$

where the scattered light intensity is corrected to the unit basis of the incident light intensity, and I_{tr}^{raw} and $I_{s,\theta}^{raw}$ are the uncorrected transmitted light and scattered light intensities, respectively. However, this scheme does not account for the presence of background scattering that will inevitably exist due to stray lights, internal reflections, and tiny amounts of dusts. Therefore, further background subtraction is needed. For the present study, we followed a procedure proposed by Szydlowski et al. [16] and have used the following expression to obtain the final corrected scattered light intensity $I_{s,\theta,corr}(t)$ at a given scattering angle θ and time t:

$$I_{s,\theta,corr}(t) = [I_{s,\theta}(t)/I_{tr}(t)] - [I_{s,\theta}(t=0)/I_{tr}(t=0)] \quad (2)$$

Here $I_{tr}(t)$ is the transmitted light intensity and $I_{s,\theta}(t)$ is the raw data for the scattered light intensity. The second term corresponding to time zero is the measure of background scattering in the homogeneous solution prior to quench. It is this background that is subtracted in obtaining the corrected scattered light intensity.

3. Results and discussion

3.1. Demixing pressures and phase boundaries

Fig. 4(a) and (b) shows the pressure–temperature demixing curves for the two polymer samples of different molecular weights ($M_w = 50\,000$ and 700 000) at three different concentrations. In these figures, the region above each curve is the one-phase region. The negative slopes of these curves indicate that the systems display upper critical

solution temperature (UCST), that is, one-phase regions are entered upon increase in temperature.

It should be noted that the thermodynamic aspects and phase boundaries for polystyrene + methylcyclohexane systems have been studied extensively by previous researchers [43–46] also. Modeling studies have also been reported. In particular, using the mean-field lattice-gas theory [47], full description of these solutions, and detailed expressions for the interaction parameter as a function of pressure and temperature have been published [43]. We have therefore modeled the present data using the parameters available in the literature. Fig. 5 shows the pressure composition phase diagram obtained by taking constant temperature cuts from Fig. 4(a) and (b). In this figure, the solid and dashed curves are the predicted binodal and spinodal curves that were obtained using the mean-field lattice-gas theory.

In the mean-field lattice-gas theory, Gibbs free energy of mixing for polymer + solvent binary systems is expressed as

$$f_m = (1-\phi)\ln(1-\phi) + \frac{1}{r_n}\phi\ln(\phi) + g\phi\ln(1-\phi) \quad (3)$$

where ϕ is the volume fraction of the polymer, r_n the ratio of molar volume of polymer to the solvent (thus a measure of the degree of polymerization) and g is the interaction parameter which depends on temperature T, pressure P and concentration. The interaction parameter for the present system is given as $g = g_0(T,\phi) + g_1(T,P)$ with $g_0 = (a + b(T)/(1-c\phi))$ [43]. This leads to the final expressions for the chemical potentials for the solvent (μ_0) and the polymer (μ_1):

$$\mu_0 = \ln\phi_0 + \left(1-\frac{1}{r_n}\right)\phi + \left(g_1 + a + \frac{b(1-c)}{(1-c\phi)^2}\right)\phi^2 \quad (4)$$

$$\mu_1 = \ln\phi - r_n\left(\frac{\phi}{r_n} + \phi_0\right) + \left(g_1 + a + \frac{b}{(1-c\phi)^2}\right)r_n\phi_0^2 \quad (5)$$

where ϕ_0 is the solvent volume fraction. The specific expressions for g_1 and g_0 for polystyrene + methylcyclohexane systems are given by [43]

$$g_0(T,\phi) = \left(-0.1091 + \frac{-0.5832 + 278.6/T + 1.695\times10^{-3}T}{1-0.2481\phi}\right) \quad (6)$$

$$g_1(T,P) = \frac{0.434}{T}(1-0.00394T)\{P - 0.0823 \times (1-0.00298T)P^2\} \quad (7)$$

These equations have been used in the flash-point algorithm employed in the numerical calculations, i.e. at a given T and P, the two coexisting compositions have been calculated by equating the chemical potentials of the same component in both phases. For a binary system, this requires solving the following two equations simultaneously:

$$\ln\phi_0' + \left(1-\frac{1}{r_n}\right)\phi_1' + \left(g_1 + a + \frac{b(1-c)}{(1-c\phi_1')^2}\right)\phi_1'2 = \ln\phi_0'' + \left(1-\frac{1}{r_n}\right)\phi_1'' + \left(g_1 + a + \frac{b(1-c)}{(1-c\phi_1'')^2}\right)\phi_1''2 \quad (8)$$

and

$$\ln\phi_1' - r\left(\frac{\phi_1'}{r} + \phi_0'\right) + \left(g_1 + a + \frac{b}{(1-c\phi_1')^2}\right)r\phi_0'2 = \ln\phi_1'' - r\left(\frac{\phi_1''}{r} + \phi_0''\right) + \left(g_1 + a + \frac{b}{(1-c\phi_1'')^2}\right)r\phi_0''2 \quad (9)$$

where ($'$) and ($''$) quantities refer to the polymer lean and polymer rich phases.

The results are presented as the binodal predictions in Fig. 5. For nearly monodisperse polymers, the demixing pressures represent the binodal (or the coexistence) curve shown in the figure. The spinodal boundary separates the thermodynamically unstable region (inside spinodal) from the metastable region (the region between the binodal and spinodal). The binodal and the spinodal boundaries merge at the critical polymer concentration where the metastable region is eliminated. Information on the critical concentration is therefore useful in conducting phase separation studies. The critical polymer concentrations for polystyrene + methylcyclohexane solutions have been reported in the literature for a range of molecular weights [44]. Using the literature information, for the specific molecular weight polymer (M_w = 700 000 and 50 000) used in the present study, we estimate the critical concentrations to be 5.5 and 14.8% by mass, respectively. These are displayed by the model predictions in Fig. 5. It should be noted that as in Fig. 5, most model calculations for polymer solutions will predict a sharper curvature for the phase boundary near the critical concentration, and fail to describe the experimental phase boundary data that display a much flatter concentration profile.

Phase separations can be conducted by a reduction in pressure at different concentrations. If phase separation is conducted at the critical polymer concentration, then one expects that the phase separation will proceed by spinodal decomposition irrespective of the quench depth, or quench rate. However on either side of the critical concentration, it is not possible to enter the spinodal region unless the pressure quench depth is greater than some characteristic value which will depend on the actual polymer concentration. Also, at off critical concentrations, quench must be carried out relatively fast so that the phase separation does not proceed to any appreciable degree while traversing the

Table 1
Polystyrene + methylcyclohexane solutions on which pressure quench experiments have been conducted (critical polymer concentrations estimated from literature data [44] are: $M_w = 700\,000$; $C_{crit} = 5.5\%$ by mass $M_w = 50\,000$; $C_{crit} = 14.8\%$ by mass)

Solution #	Polymer molecular weight (M_w)	Concentration (% by mass)	Nominal temperature (K)
1	700 000	5.5	326
			331
2	700 000	9.6	326
			331
3	50 000	4.6	309
4	50 000	10.4	311
5	50 000	15.9	309
			311
			313

metastable region. It is here that the multiple rapid repetitive pressure-quench (MRPD) methodology becomes attractive. Starting at a point such as point **a** in Fig. 5 in the one phase region, pressure is rapidly reduced to a lower value, i.e. corresponding to point **b** and the time evolution of scattered light intensities are monitored. Then the pressure is brought back to **a** and a deeper quench is imposed with an end pressure, corresponding to point **c**. Once again scattered light intensities are monitored. Whether the phase separation proceeds by nucleation and growth or spinodal decomposition is assessed by the time evolution (i.e. the kinetics) of the angular dependence of the scattered light intensities which, in the case of spinodal decomposition, displays a scattering maximum that grows with time.

In the present study, we have conducted pressure quench experiments at both the critical and off-critical polymer concentrations for the two molecular weight samples. Table 1 is a summary of all the quench experiments conducted. Solutions #1 is at the critical polymer concentration (5.5%) for $M = 700\,000$ as reported in the literature. Solution #5 is very close to the literature value of the critical concentration (14.8%) for $M = 50,000$, and due to the flat nature of the phase boundary near the critical point may be treated as being at the critical concentration. Solutions # 2 ($M = 700\,000$) and solutions #3 and #4 ($M = 50\,000$) are at off-critical concentrations. The results are discussed below in the following sections.

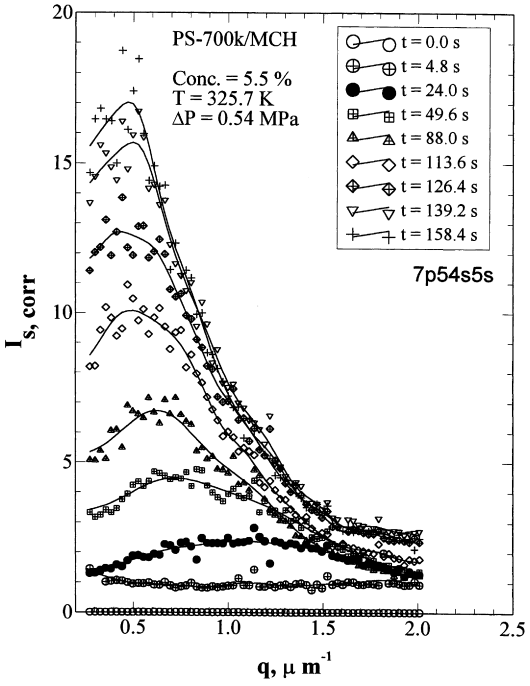

Fig. 6. Scattered light intensity profiles as a function of wave number (scattering angle) and time for a pressure quench in 5.5% by mass polystyrene ($M_w = 700\,000$) solution in methylcyclohexane at 325.7 K. The quench depth $\Delta P = 0.54$ MPa. The elapsed time before the pressure quench has been subtracted to give the actual duration of phase separation for each curve.

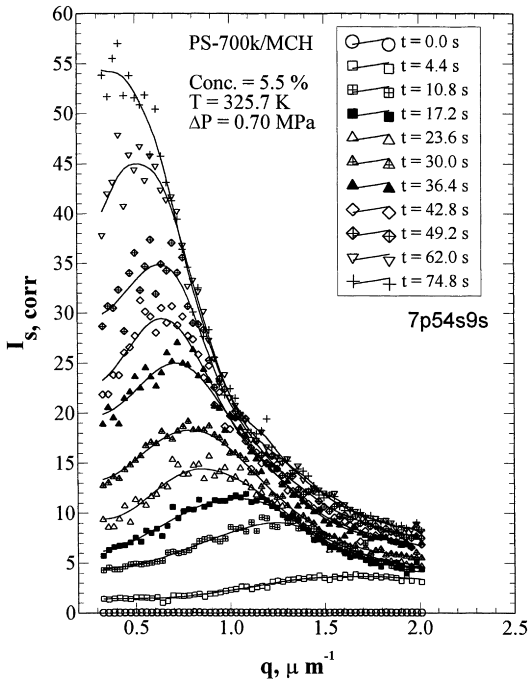

Fig. 7. Scattered light intensity profiles as a function of wave number (scattering angle) and time for a pressure quench in 5.5% by mass polystyrene ($M_w = 700\,000$) solution in methylcyclohexane at 325.7 K. The quench depth $\Delta P = 0.70$ MPa. The elapsed time before the pressure quench has been subtracted to give the actual duration of phase separation for each curve.

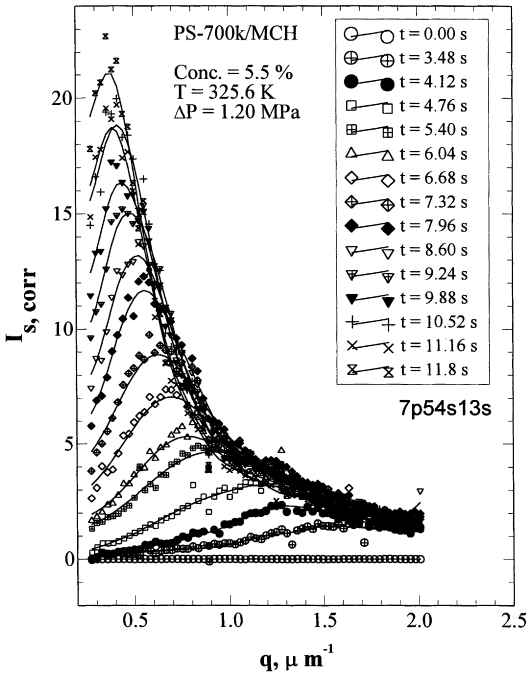

Fig. 8. Scattered light intensity profiles as a function of wave number (scattering angle) and time for a pressure quench in 5.5% by mass polystyrene ($M_w = 700\,000$) solution in methylcyclohexane at 325.6 K. The quench depth $\Delta P = 1.20$ MPa. The elapsed time before the pressure quench has been subtracted to give the actual duration of phase separation for each curve.

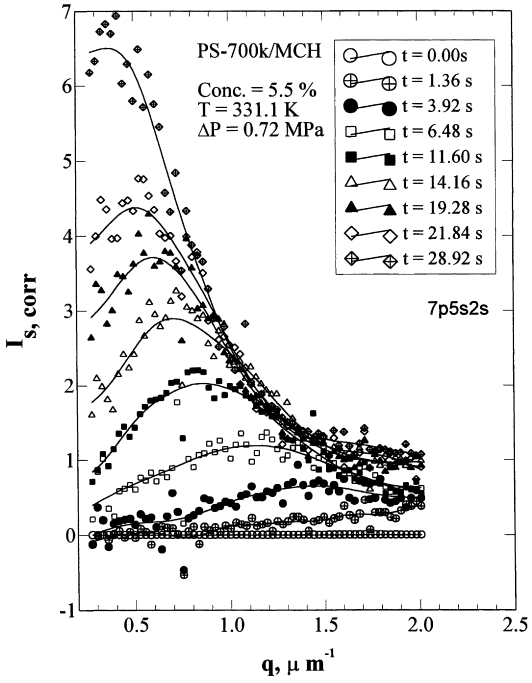

Fig. 9. Scattered light intensity profiles as a function of wave number (scattering angle) and time for a pressure quench in 5.5% by mass polystyrene ($M_w = 700\,000$) solution in methylcyclohexane at 331.1 K. The quench depth $\Delta P = 0.72$ MPa. The elapsed time before the pressure quench has been subtracted to give the actual duration of phase separation for each curve.

3.1.1. Critical quenches

The general features of the evolution of the scattered light intensity for critical quenches are illustrated in Figs. 6–8 for the 5.5% solution of the high molecular weight polymer sample ($M = 700\,000$, solution #1) at 325.7 K for quench depths of 0.54, 0.70, and 1.20 MPa, respectively. The figures show the corrected scattered intensities as a function of the angle (θ) expressed in terms of the wave vector (q) which is equal to $(4\pi n_0/\lambda)\sin(\theta/2)$. Here, λ is the wave length of the laser light in vacuum and n_0 is the refractive index of the media. (In the present study, the refractive index was taken to be that of methylcyclohexane, neglecting the corrections due to polymer concentration or pressure which would slightly alter the actual q values, but does not alter the general trend.)

For all quenches, a maximum in the scattered light intensity profile is observed to develop shortly after the quench. In all the cases, scattered light intensity maximum (I_m) increases with time and its position q_m shifts to lower q values until it coincides with the transmitted light, and becomes indistinguishable from the forward beam. These features are the characteristics of spinodal decomposition. The physical observation of the intensity maximum is a consequence of the formation of domain structures with some degree of regularity throughout the system during the phase separation process. These data show that such regularity starts and develops rather quickly (within seconds) in these solutions, which is in contrast to very viscous systems such as polymer blends. Further, in contrast with the common behavior observed in polymer blends for which the q_m remains constant for some initial time interval following the quench (with its value remaining as that at $t = 0$), in the present system there is no clearly identified early time interval in which q_m is stationary. The early time may be limited to extremely short times, being in the time scale of ms or μs. The elapsed time before the wave number corresponding to the maximum scattered light intensity shifts out of experimental q range, is in the range from 8 to 160 s (for the deepest and shallowest quenches, respectively) and can be taken as an indicator for the full duration of phase separation.

Comparison of Figs. 6–8 show that the spinodal decomposition proceeds faster for the system subjected to deeper pressure quenches.

The evolution of the scattered light intensity for this 5.5% solution at the higher temperature of 331 K has the same qualitative features but the duration of phase separation becomes shorter compared to 326 K. As an example, this is demonstrated in Fig. 9 for the quench with $\Delta P = 0.72$ MPa. The duration of phase separation before the intensity maximum moves beyond the beam stop is about 29 s which is much shorter that 75 s (Fig. 7) observed for a similar quench ($\Delta P = 0.70$ MPa) at the lower temperature 326 K. The faster kinetics that are observed at the higher temperature is more likely to be the consequence of the lower viscosities displayed at higher temperatures. The

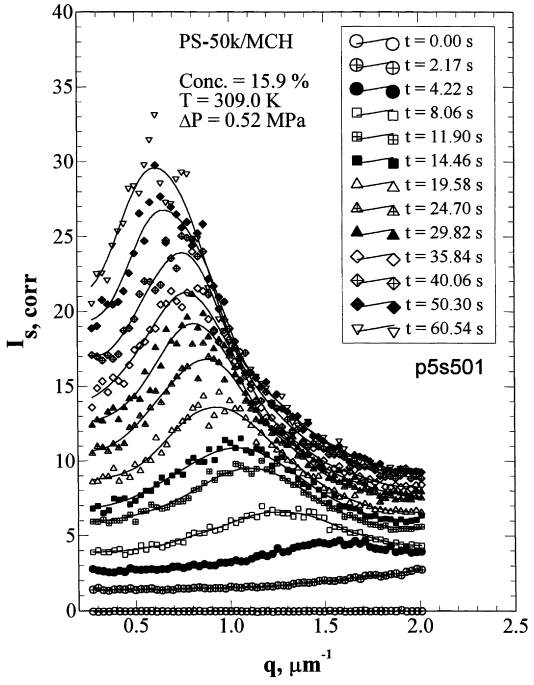

Fig. 10. Scattered light intensity profiles as a function of wave number (scattering angle) and time for a pressure quench in 15.9% by mass polystyrene ($M_w = 50\,000$) solution in methylcyclohexane at 309.0 K. The quench depth $\Delta P = 0.52$ MPa. The elapsed time before the pressure quench has been subtracted to give the actual duration of phase separation for each curve.

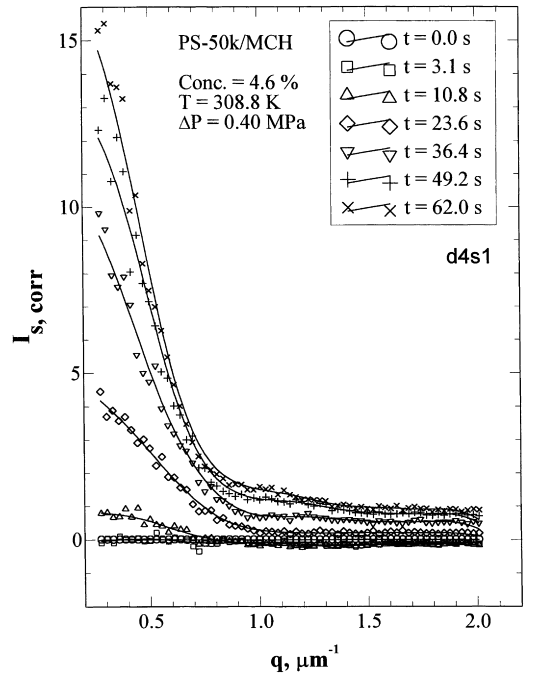

Fig. 11. Scattered light intensity profiles as a function of wave number (scattering angle) and time for a pressure quench in 4.6% by mass polystyrene ($M_w = 50\,000$) solution in methylcyclohexane at 308.8 K. The quench depth $\Delta P = 0.40$ MPa. The elapsed time before the pressure quench has been subtracted to give the actual duration of phase separation for each curve.

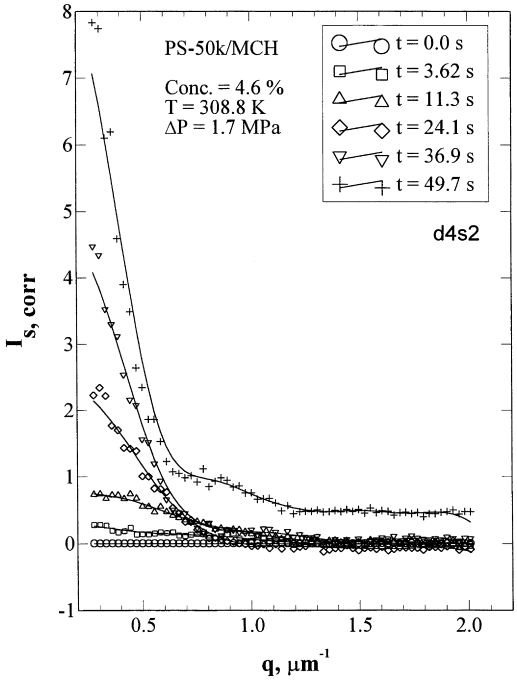

Fig. 12. Scattered light intensity profiles as a function of wave number (scattering angle) and time for a pressure quench in 4.6% by mass polystyrene ($M_w = 50\,000$) solution in methylcyclohexane at 308.8 K. The quench depth $\Delta P = 1.7$ MPa. The elapsed time before the pressure quench has been subtracted to give the actual duration of phase separation for each curve.

recent viscosity measurement [48] shows that a 5% polystyrene solution ($M = 700\,000$) in methylcyclohexane undergoes about 15% viscosity reduction upon an increase in temperature from 360 to 380 K. At 326 K, a unit increase in temperature is expected to result in a greater viscosity reduction than at 380, and the viscosity reduction with a 5 K temperature difference can be significant. Indeed, using the reported flow activation energy value of 8.55 kJ/mol at 15 MPa, for 5% solution, the viscosity reduction in going from 326 to 331 K is estimated to be about 5%.

For the 15.9% solution of the lower molecular weight polymer sample ($M = 50\,000$, solution #5) which is very close to the critical concentration for this molecular weight, the qualitative features remain the same. Fig. 10 is a representative example of the evolution of the scattered light intensity for this solution at a quench depth of $\Delta P = 0.52$ MPa at $T = 309.0$ K. A reliable indicator to compare the phase separation times is to compare the time for the I_m to be observed at the same q value. Comparison with results obtained for the critical quench data for the high molecular weight sample of similar quench depth (see Fig. 6) show that the phase separation process is proceeding faster with the lower molecular weight polymer sample. If conducted at the same temperature, the contrast would be even more significant.

3.1.2. Off-critical quenches

Depending upon the concentration and the molecular

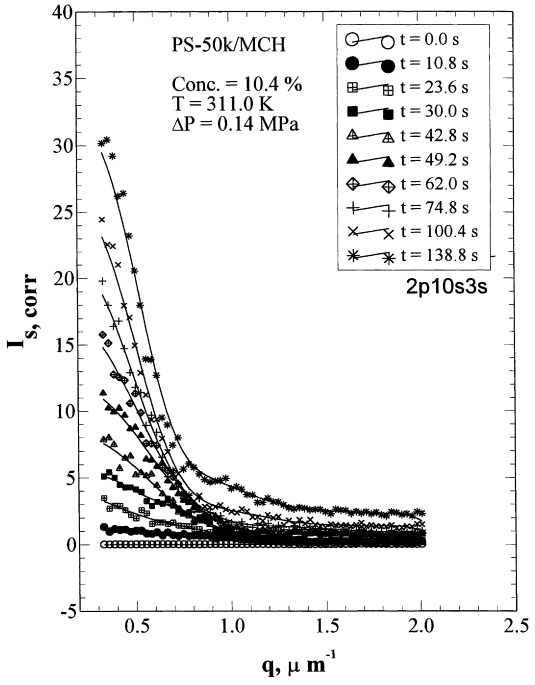

Fig. 13. Scattered light intensity profiles as a function of wave number (scattering angle) and time for a pressure quench in 10.4% by mass polystyrene ($M_w = 50\,000$) solution in methylcyclohexane at 311.0 K. The quench depth $\Delta P = 0.14$ MPa. The elapsed time before the pressure quench has been subtracted to give the actual duration of phase separation for each curve.

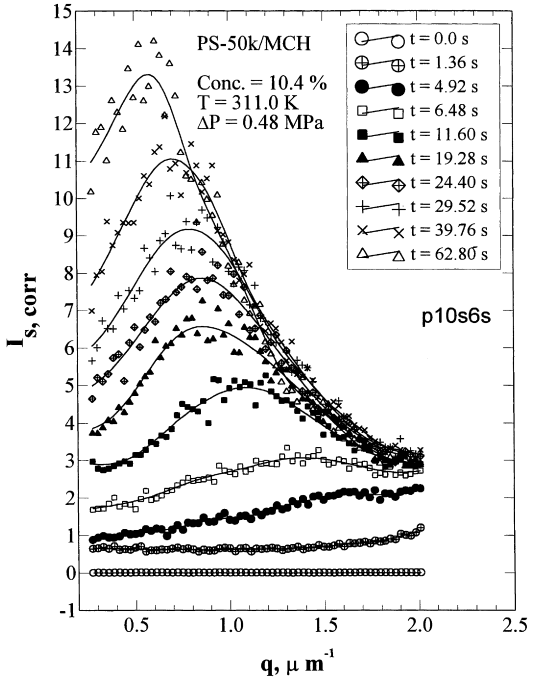

Fig. 14. Scattered light intensity profiles as a function of wave number (scattering angle) and time for a pressure quench in 10.4% by mass polystyrene ($M_w = 50\,000$) solution in methylcyclohexane at 311.0 K. The quench depth $\Delta P = 0.48$ MPa. The elapsed time before the pressure quench has been subtracted to give the actual duration of phase separation for each curve.

weight, solutions at off-critical concentrations were observed to display different features in the scattered light intensity profiles.

Fig. 11 shows the evolution of the scattered light intensity for the low molecular weight polymer sample ($M = 50\,000$, Solution #3) at a relatively low concentration (4.6%) compared to the critical polymer concentration (14.8%) at 308.8 K. The quench depth is $\Delta P = 0.4$ MPa. No maximum in the scattered light intensity profile is observed. For this solution, maximum in the scattered light intensity profile could not be observed for much deeper quenches (up to $\Delta P = 1.7$ MPa, Fig. 12) either. The absence of the scattering maximum is a characteristic of phase separation by nucleation and growth. Quenches deeper than 1.7 MPa were not conducted for this solution. The absence of a maximum in the scattered light intensity profile may sometimes be a result of the limited q range in the measurements. For example, in the studies of spinodal decomposition using shorter wavelength radiation (X-ray [9] or Neutron scattering [49]), the characteristic peak of spinodal decomposition may be missed due to the higher q range. In those experiments, similar scattering profiles with apparent monotonic trend as shown in Figs. 11 and 12 is observed, while in fact the peak lies outside the accessible q range. However, this should not be the case here. This is because the wavelength of the concentration fluctuations that we are able to monitor is larger by several orders of magnitude than the radius of gyration of the polymer or the correlation length which should be comparable to the wavelength of the initial peak position if it exists. Therefore, such monotonic decrease of the scattered light intensity with q appears to indicate that nucleation and growth mechanism dominates the phase separation for these quenches.

When the concentration is increased to 10.4% (solution #4, Table 1), the scattering pattern was found to vary with the quench depth. For shallow quenches, there is no maximum observed in the scattered light intensity profile. Fig. 13 shows the scattered light intensity as a function of q for $\Delta P = 0.14$ MPa at 311.0 K. No maximum was observed for quenches up to 0.4 MPa. However, for quenches with $\Delta P > 0.4$ MPa, a maximum in the scattered light intensity profile is observed. This is shown in Fig. 14 for a quench-depth of $\Delta P = 0.48$ MPa. These observations suggest that the metastable gap for this solution is about 0.4 MPa, and different mechanisms, i.e. nucleation and growth vs. spinodal decomposition, takes place in the metastable and the unstable region. These observations also suggest that, by using a relatively fast pressure quench, the metastable region can be crossed and the unstable two-phase region can indeed be entered without causing substantial amount of nucleation.

The behavior at a concentration above the critical concentration is illustrated in Figs. 15 and 16 for 9.6% solution of the higher molecular weight polymer ($M = 700\,000$; Solution #2) at 330.7 K for quench depths of $\Delta P = 0.30$ and 0.80 MPa. Spinodal decomposition was observed for

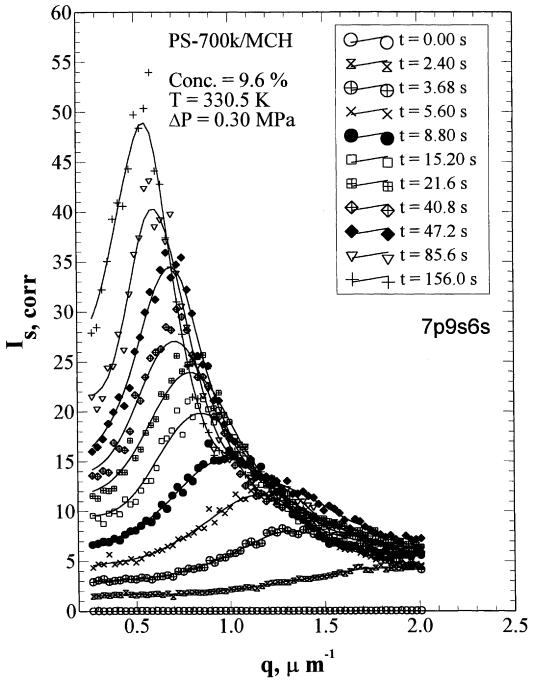

Fig. 15. Scattered light intensity profiles as a function of wave number (scattering angle) and time for a pressure quench in 9.6% by mass polystyrene ($M_w = 700\,000$) solution in methylcyclohexane at 330.5 K. The quench depth $\Delta P = 0.30$ MPa. The elapsed time before the pressure quench has been subtracted to give the actual duration of phase separation for each curve.

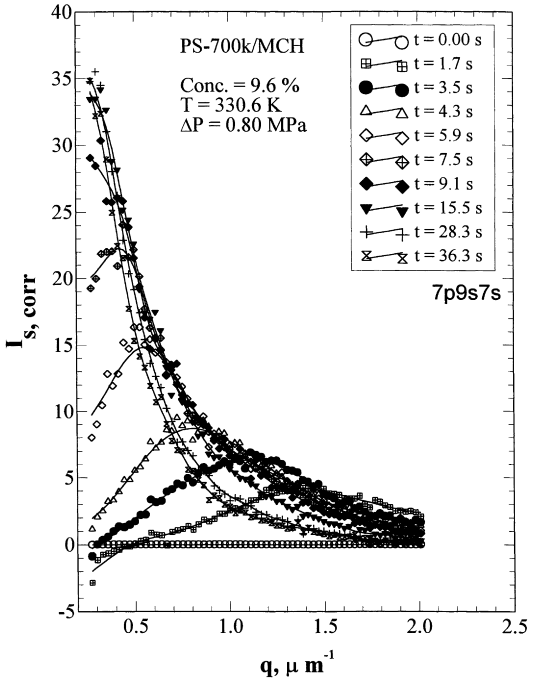

Fig. 16. Scattered light intensity profiles as a function of wave number (scattering angle) and time for a pressure quench in 9.6% by mass polystyrene ($M_w = 700\,000$) solution in methylcyclohexane at 330.6 K. The quench depth $\Delta P = 0.80$ MPa. The elapsed time before the pressure quench has been subtracted to give the actual duration of phase separation for each curve.

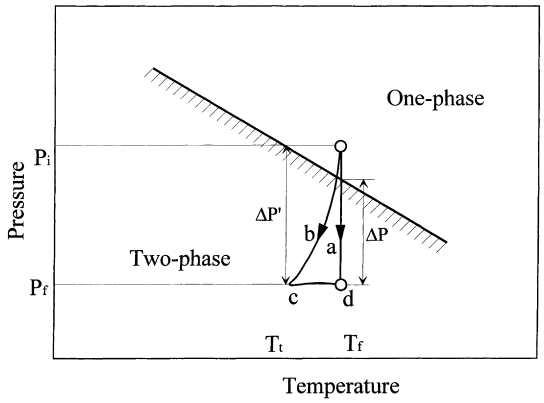

Fig. 17. Schematic diagram of the isothermal (a) and the actual (b) quench paths during a pressure-quench experiment from an initial pressure of P_i to a final pressure of P_f. The system experiences a nearly adiabatic cooling following path b before it equilibrates to the initial temperature.

even deeper quenches tested up to 1.2 MPa for this system. The metastable gap for this solution may be shallower than 0.3 MPa. However, this aspect was not further investigated. It should be noted that, as before, with deeper quenches, phase separation time becomes shorter. A distinct feature displayed in Fig. 16 is the crossing of the scattered light intensities at high q range with time which is a result of the spinodal ring moving to lower q values.

Some experiments for the high molecular weight polymer sample at 3.0% concentration, a concentration below the critical concentration, showed that phase separation proceeds by nucleation and growth for a quench depth of 0.13 MPa, but by spinodal decomposition for a quench depth of 0.69 MPa and higher. The exact location of the spinodal crossover was not determined at this time. This is in contrast to the lower molecular weight polymer for which at 4.6% spinodal decomposition could not be observed up to a quench depth of 1.7 MPa that was investigated.

3.2. Further discussion

3.2.1. Quench path

It is important to recognize the complex nature of the actual quench path in these experiments. This is due to the complex temperature and pressure profile during the quench.

As demonstrated in Fig. 3, pressure quench is accompanied with a temperature drop. As the negative slope of the PT curves (Fig. 4), the actual quench path, if only measured by the pressure difference would be larger than the apparent quench depth before the temperature is completely restored to its initial value. This is demonstrated in Fig. 17. As shown, the quench $\Delta P'$ experienced at point c at a lower temperature T_t would be deeper than the quench ΔP at point d at the final temperature T_f.

In Figs. 6–16, the indicated temperatures correspond to the nominal temperature. However, in all experiments, the temperature recovers after initial reduction was completed

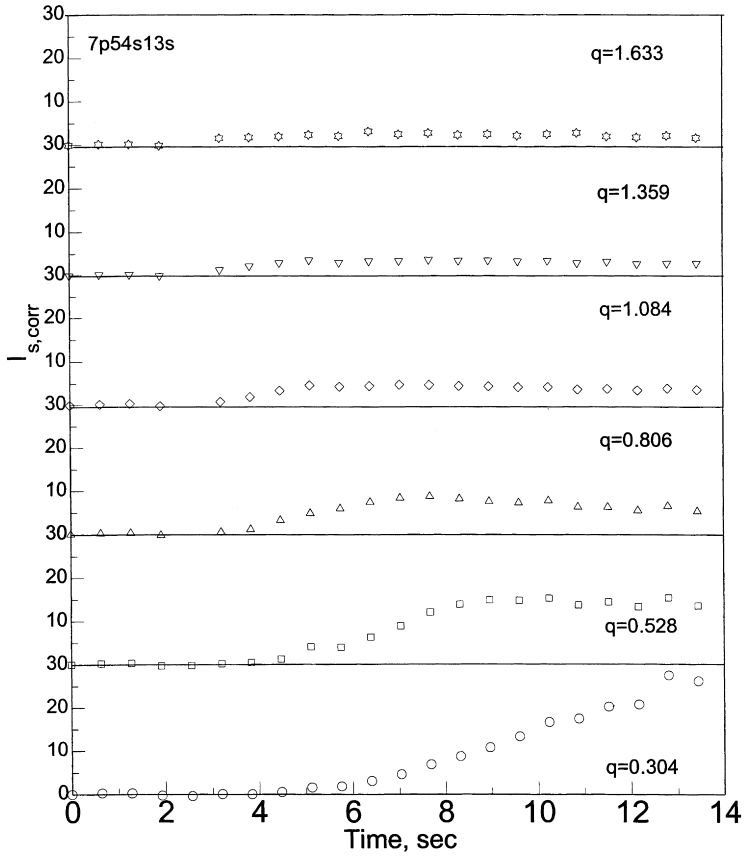

Fig. 18. Evolution scattered light intensity as a function of time after phase separation. Experimental conditions are given in Fig. 8.

within 2 s for most quenches within $\Delta P < 1$ MPa and within 5 s for the deeper quenches [50], and the scattering profile that are shown in the figures do indeed represent the progress at isothermal conditions.

3.2.2. Early stage of pressure-induced spinodal decomposition

For systems undergoing spinodal decomposition the linearized Cahn–Hilliard theory [22–25] predicts an exponential growth for the scattered light intensity, i.e.

$$I_s(q,t) \sim e^{2R(q)t} \tag{10}$$

where $R(q)$ is the rate of growth of concentration fluctuations given by

$$R(q) = D_{app}q^2[1 - (q^2/2q_{m0}^2)] \tag{11}$$

where D_{app} is the apparent diffusivity, and q the wave number of the growing fluctuations as defined before, q_{m0} is the time-invariant initial wave number corresponding to the maximum growth rate of fluctuations corresponding to time $t = 0$.

Fig. 18 shows the growth of the scattered light intensity at several selected q values for 5.5% solution ($M_w = 700\,000$) at 325.6 K after a quench of 1.20 MPa. As shown in this figure, for small wavenumbers (i.e. $q = 0.304$), scattered light intensity increases during the full observation period of 14 s. For larger q values, however, the scattered light intensity rises quickly at first, reaches a maximum, and then decreases. The time it takes to reach the maximum becomes shorter as q becomes larger, which is a consequence of coarsening of the small domains.

Fig. 19 is a semi-log plot of the data shown in Fig. 18 to help identify if there is an early stage region where the light intensity variation is as would be anticipated by the Cahn–Hilliard theory (Eq. (10)). By taking the linear portion of the data, the growth rate $R(q)$ can be calculated from the slopes. Eq. (11) would then permit determination of the diffusion coefficient from

$$D_{app} = \lim_{q\to 0} R(q)/q^2 \tag{12}$$

For reasonable evaluation of D_{app}, information on q_{m0} is also needed which however has not been experimentally accessible in the present study. A direct approach to evaluate q_{m0} is to revert to one of the basic relationships in the Cahn–Hilliard theory which provides an explicit expression for q_{m0} as

$$q_{m0} = \sqrt{\frac{D_{app}}{2M\kappa}} = \sqrt{-\frac{1}{2\kappa}\frac{\partial^2 f_m}{\partial \phi^2}} \tag{13}$$

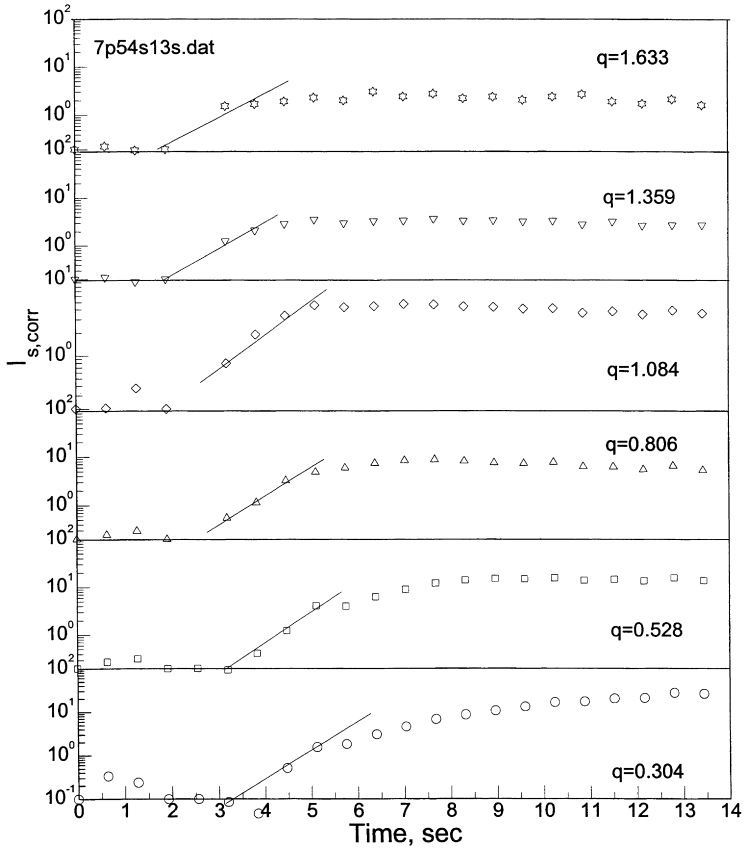

Fig. 19. Evolution of scattered light intensity as a function of time at early stage of phase separation. Experimental conditions are given in Fig. 8.

where M is mobility, f_m the free energy of mixing, ϕ the volume fraction of polymer, κ the gradient energy coefficient given by $\kappa = \sigma^2/18\phi(1-\phi)$, and σ is the polymer segment length. Therefore, from the knowledge of the free energy of mixing, and the segment length (which for polystyrene can be assumed to be 0.275 nm[6]), q_{m0} can be calculated for a given solution. We have adopted this approach to evaluate q_{m0}.

For the free energy of mixing we have used the mean-field expression given by Eq. (3). As shown in Fig. 5, using this equation gives reasonable predictions of the phase boundaries. However, even though small, it must be noted that the differences in experimental data and the predictions of the phase boundaries may lead to differences in the numerical value of the quench depth assumed, and thus

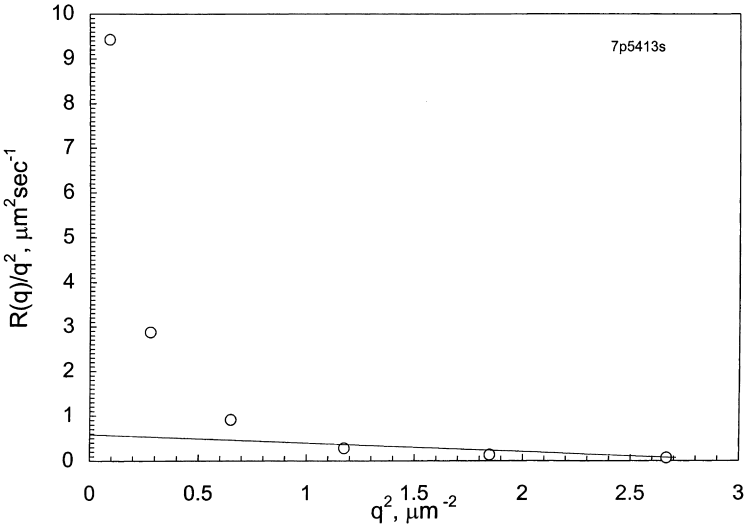

Fig. 20. Estimation of apparent diffusivity from high q values from Cahn-plot.

Table 2
Characteristic parameters for 5.5% solution of polystyrene ($M = 700\,000$) in methylcyclohexane

T (K)	ΔP (MPa)	$q_m(0)$ (μm^{-1})	$D \times 10^8$ ($cm^2 s^{-1}$)[a]	τ_0 (s)	α	β
325.7	0.54	1.8	0.04	7.7	0.39	0.78
325.7	0.70	2.0	0.09	2.8	0.44	0.86
325.6	0.91	2.3	0.15	1.3	0.70	1.36
325.9	1.20	2.6	0.14	1.1	1.10	2.01

[a] As evaluated from the highest experimental q value. The values that are estimated from extrapolations from high q values similar to Fig. 20 give somewhat higher values of 0.04, 0.18, 0.28 and 0.60×10^{-8} cm^2/s for the diffusion coefficient as obtained from these quenches, respectively.

may lead to errors in the kinetic analyses. The estimate of q_{m0} is most sensitive to the quench depth, i.e. the end pressure relative to the phase boundary or spinodal curve. To make sure that the calculations are consistent, in estimation of the interaction parameter g, instead of directly using the experimentally recorded end-pressures, we used the calculated spinodal pressure minus the experimental quench depth ΔP to obtain the appropriate end pressure to use in the calculations. This way, the real quench depth is preserved in our calculations. Such procedure has been carried out for the calculation of q_{m0}, and for this polymer solution at its critical concentration a value of $q_{m0} = 2.6\ \mu m^{-1}$ has been determined. Using this value, D_{app} is evaluated to be in the range from 10^{-9} to 10^{-8} cm^2/s, which appears reasonable for the diffusion coefficient for a polymer solution. Fig. 20 is a plot of $R(q)/q^2$ versus q^2 from which extrapolation to $q = 0$ from high q values suggest 0.6×10^{-8} cm^2/s. It is important to recognize the significance of limiting this type of analysis to high q values only. Evaluation of the apparent diffusion constant from the highest value of q and the corresponding growth rate R for $q = 1.633$ (which may be a preferred method for systems in which the initial stationary stage is not discernable) gives a value of 0.14×10^{-8} cm^2/s.

Table 2 shows the values of q_{m0} and D_{app} for different quenches at the critical polymer concentration for the high molecular weight polymer solution at 325 K. The analysis of the q_{m0} values with the quench depth shows that q_{m0} varies as $\Delta P^{-0.5}$. This appears reasonable as q_{m0} is a measure of the correlation length which has a critical exponent of 0.5 along the critical isochore in the mean-field description [51]. The apparent diffusivity is also observed to show dependence with quench depth and vary as $\Delta P^{2.5}$. This is consistent with studies for polymer solutions and blends [6] subjected to temperature quench where diffusions coefficients are reported to depend on the depth of the temperature quench, and vary as $\Delta T^{0.6}$. The present study suggests a much greater sensitivity of diffusion coefficient to the pressure quench depth imposed.

For solutions at off-critical concentrations, this procedure can not be readily applied unless the exact location of the spinodal pressure is first established and is consistent with the spinodal pressure predicted by the model. The mean-field theory predicts a much wider metastable gap to permit the use of this approach for off-critical concentrations.

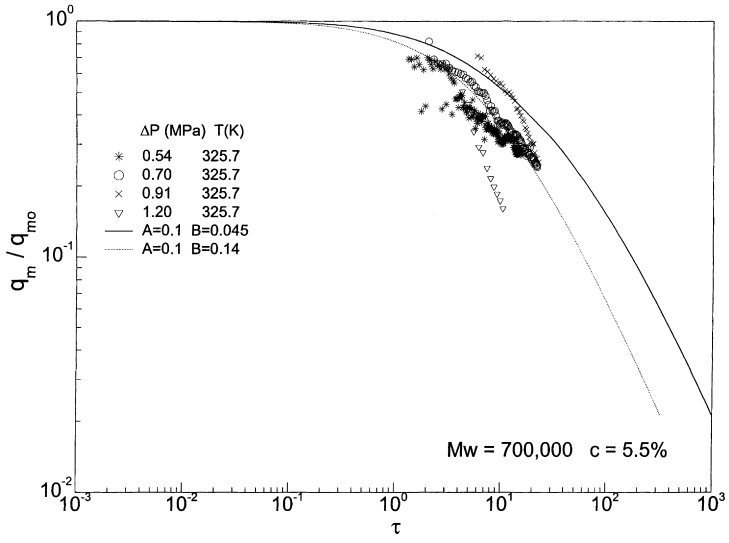

Fig. 21. Reduced wavenumber of dominant concentration fluctuation as a function of reduced time for 5.5% polystyrene solutions in methylcyclohexane with $M_w = 700\,000$. The curves are the theoretical results calculated using Furukawa scaling function with different values of parameters A and B (see text).

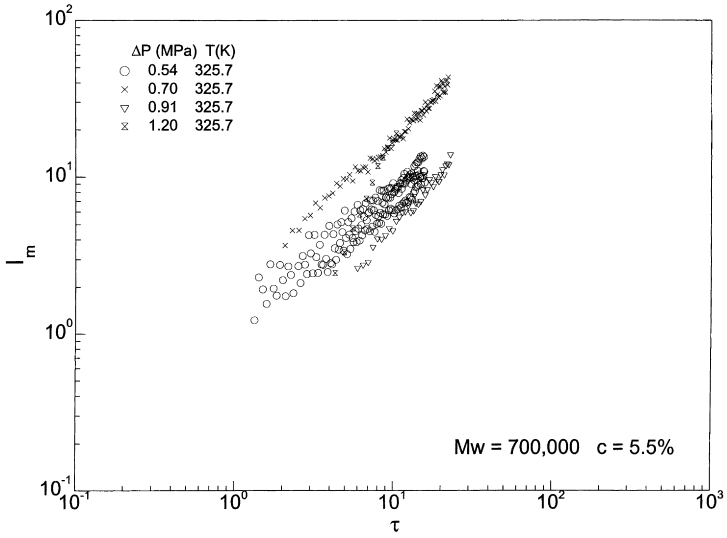

Fig. 22. Maximum scattered light intensity as a function of reduced time for 5.5% polystyrene solutions in methylcyclohexane with $M_w = 700\,000$.

3.2.3. Intermediate and late stage of spinodal decomposition

At intermediate stage, both the amplitude and wavenumber of concentration fluctuations change with time. At the late stage, sharp interfaces are developed between phase domains. While the domain size may keep increasing, the concentration inside the domain is close to the corresponding equilibrium concentration. At this stage, power law approximations for both the maximum in the scattered light intensities I_m and its wavenumber q_m are often used [1,6] to characterize the rate of coarsening in accordance with the following relationships:

$$Q_m = \frac{q_m}{q_{m0}} \sim \tau^{-\alpha} \tag{14}$$

and

$$I_m \sim \tau^{\beta} \tag{15}$$

where τ is the reduced time

$$\tau = \frac{t}{\tau_0} \tag{16}$$

and τ_0 is defined as

$$\tau_0 = \frac{1}{D_{app} q_{m0}^2} \tag{17}$$

For the 5.5% solution of high molecular weight polymer, the calculated values of τ_0 are also given in Table 2. Using the characteristic length $1/q_{m0}$ and the characteristic time τ_0 values given in Table 2, we have tested the validity of these power law relationships. Fig. 21 shows the double logarithmic plot q_m/q_{m0} vs τ at 325.7 K. The linear fits for these data sets have been used to determine the values of exponent α which are tabulated in Table 2. The general observation for fluid systems undergoing phase separation from previous investigations [6,28,29] is rather simple. The peak position q_m decays slowly at first, and as the reduced time elapses, the decay rate gradually increases from about 1/3 at the intermediate stage to a value of about 1.0 at the late stage. The change of q_{m0} over a large reduced time scale has been summarized by Furukawa [27] who for fluid systems has proposed the following scaling relationship of q_{m0} vs τ:

$$B\tau = \left(\frac{q_m(0)}{q_m} - 1\right) - \left\{\left(\frac{A}{B}\right)^{1/2}\left[\tan^{-1}\left(\frac{q_m(0)}{q_m}\left(\frac{B}{A}\right)^{1/2}\right) - \tan^{-1}\left[\left(\frac{B}{A}\right)^{1/2}\right]\right]\right\} \tag{18}$$

This has been plotted in Fig. 21 with values of $A = 0.1$ and $B = 0.045$ which are known to describe the experimental results in small molecule fluid mixtures [27], and with $A = 0.1$ and $B = 0.14$ which were found to be effective in characterizing polydimethylsiloxane + diethyl carbonate system [5]. The present data sets are better described as expected with parameters for a polymer system. The plot in Fig. 21 suggests that the present data sets correspond mostly to the intermediate stage of spinodal decomposition for these solutions. The numerical value of α ranges from 0.39 to 1.1, the value increasing with the increased quench depth. For the shallower quenches, α is very close to 1/3, but for deep quenches, becomes larger, approaching 1, which is as predicted by Siggia [52].

Fig. 22 shows the power law dependence of I_m on τ for the same solution at 325.7 K for different quenches. The slopes give the β values that are tabulated in Table 2. The values are in the range from 0.8 to 2.0. According to the scaling argument [53], at early to intermediate stage the exponents α and β should satisfy the relationship $\beta > 3\alpha$, while in the

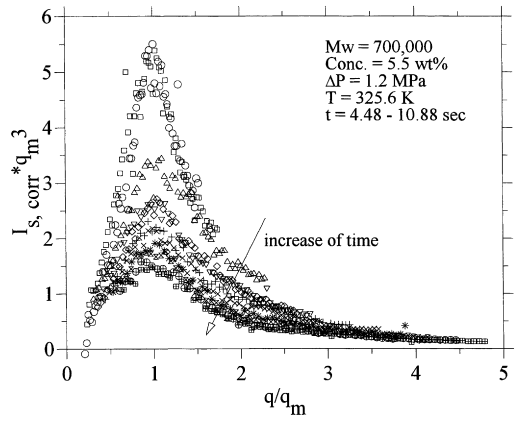

Fig. 23. Test of dynamic scaling hypothesis for the reduced structure factor for a critical quench. The data correspond to that shown in Fig. 8. Dimensionality $d = 3$ is used in the scaling calculation.

late stage $\beta = 3\alpha$. As shown in Table 2, for the present system $\beta \approx 2\alpha$. A similar relationship has been reported for some other polymer solutions in the literature [6] and is often attributed to hydrodynamic features. The $\beta \approx 2\alpha$ dependence suggests a dimensionality of 2 rather than 3 for the present system that could also probably be indicative of the non-spherical domain growth. Recent studies [54] on the kinetics of pressure-induced phase separation in solutions of polydimethylsiloxane in supercritical carbon dioxide also give the $\beta \approx 2\alpha$ dependence.

3.2.4. Scaling analysis of structure factor

In systems where dynamic similarity prevails, towards the late stage of phase separation the domain structures grow by simple enlargement, while their morphology remains the same. The scattered light intensity is a direct measurement of dynamic scaling for structure factor. Scaling analysis suggests that the scattered light intensity when normalized with a characteristic volume at a given time

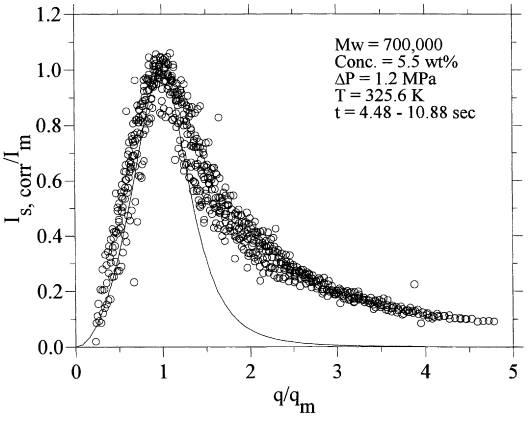

Fig. 24. Test of dynamic scaling hypothesis for the reduced structure factor for a critical quench. The solid curve is calculated using Furukawa universal scaling function $F(x) = 4x^2/(3 + x^8)$. Apparent dimensionality $d = \beta/\alpha$ is used in the scaling calculation.

would scale with $q/q_m(t)$, that is

$$I_s(q,t)/L^d(t) \sim F(q/q_m(t)) \tag{19}$$

where $1/q_m(t)$ is often the characteristic length scale $L(t)$ in scaling expression. Furukawa [27] has proposed the following scaling formalism for critical and off-critical quenches:

$$F(x) = 4x^2/(3 + x^8) \qquad \text{(critical quench)} \tag{20}$$

$$F(x) = 3x^2/(2 + x^6) \qquad \text{(off-critical quench)} \tag{21}$$

where $x = q/q_m(t)$. The asymptotic behavior of these functions are

$$F \sim x^2 \qquad \text{for } x \ll 1 \tag{22}$$

$$F \sim x^{-6} \qquad \text{for } x \gg 1 \tag{23}$$

for critical quench, and

$$F \sim x^{-4} \qquad \text{for } x \gg 1 \tag{24}$$

for off-critical quench.

We have tested the applicability of Furukawa scaling theory with our data. We choose $1/q_m(t)$ as the characteristic length scale $L(t)$. If one were to assume that the dimensionality were 3, then plots of $I_s q_m^3$ should scale with q/q_m. As a representative example for the critical quench, Fig. 23 shows such a plot for the late stage behavior following the 1.20 MPa quench in 5.5% solution ($M_w = 700\,000$). As shown, the normalized scattered light intensities do not collapse to a master curve. Similar behavior has been observed for other quenches with this solution. In a way, this was somewhat expected. From the power law analysis about the growth rate of q_m and I_m as discussed earlier, the relationship between the two exponents $\beta = 3\alpha$ does not hold for the present data implying that the apparent dimensionality of the system is not 3. Power law analysis of our data suggested a dimensionality of 2 that would suggest plotting $I_s q_m^2$ versus q/q_m to test universal scaling. But a better approach applicable to the present data is to use the apparent dimensionality given as $d = \beta/\alpha$. Eq. (19) in combination with Eqs. (14) and (15) imply that

$$I_s(q,t)/L^d(t) \sim I_s(q,t)q_m^d \sim I_s(q,t)/(t^\alpha)^d \sim I_s(q,t)/t^\beta \sim I_s(q,t)/I_m \tag{25}$$

or

$$I_s(q,t)/I_m \sim F(q/q_m(t)) \tag{26}$$

We have used this scaling relationship to test the experimental data. Fig. 24 shows the results for the same initial data that was used in Fig. 23. As shown in this figure, I_s/I_m collapses rather well to a master curve. Similar to the present approach, better collapse of data with $d = 2$ have been reported for other systems [6]. Near the peak position, i.e. $q/q_m = 1$, the match between the experimental data and the theoretical Furukawa curve (Eq. (20)) appears good, but

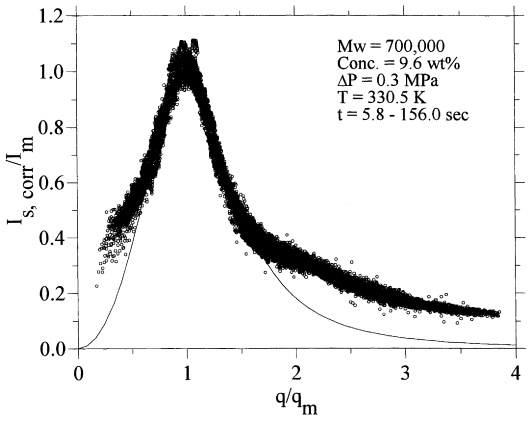

Fig. 25. Test of dynamic scaling hypothesis for the reduced structure factor for an off-critical quench. The solid curve is calculated using Furukawa universal scaling function $F(x) = 3x^2/(2 + x^6)$. Apparent dimensionality $d = \beta/\alpha$ is used in the scaling calculation.

deviations are observed for $q \gg_m$. For this particular quench, we do not see the asymptotic q^{-6} behavior at the limit of $q/q_m \gg 1$.

Fig. 25 shows the scenario for an off-critical quench for 9.6% solution of high molecular weight polymer. The quench depth is 0.3 MPa and the temperature is 330.5 K. Similar to the critical quench, the data do not collapse if a dimensionality of $d = 3$ is used but with dimensionality of $d = \beta/\alpha, I_s/I_m$ collapse to a master curve as shown. Here also discrepancies with Furukawa scaling function (Eq. (21)) are observed for $q \ll_m$ or $q \gg_m$. We do not see the asymptotic q^{-4} behavior at the limit of $q/q \gg_m 1$. This suggests that the interface between the domains are probably still diffuse. (Systems which show q^{-4} dependence are known to display sharp interface between the domains [55]). Another discrepancy with Furukawa scaling is the occurrence of a shoulder near $q/q_m = 2$. In a study of spinodal decomposition in polymer solutions, Kuwahara et al. [5] also reports a secondary peak at high q numbers which is observed in addition to the primary peak. With the evolution of the phase separation, the secondary peak can become a shoulder. Large mismatch with the Furukawa's scaling function was also reported in another study [6]. It may be that this shoulder in Fig. 25 is a manifestation of a secondary peak in our experiments representative of a secondary structure which may have evolved rapidly and merged with the primary peak.

4. Conclusion

Time-resolved small angle light scattering experiments can be used to differentiate and identify the crossover from nucleation and growth to spinodal decomposition in polymer solutions subjected to a pressure quench. In solutions of polystyrene + methylcyclohexane at the critical concentration, the phase separation proceeds exclusively via spinodal decomposition for shallow or deep quenches. However, phase separation proceeds faster for deeper quenches. For off-critical solutions, phase separation proceeds by nucleation and growth for shallow quenches, and there is a crossover to spinodal decomposition for deeper quenches.

Kinetics of of phase separation shows a non-linear phase growth, and a stationary q_{m0} is not observed experimentally. Apparent diffusivity calculations based on the estimated values of q_{m0} resulted in values in the range of 10^{-8}–10^{-9} cm^2/s. Apparent diffusivity was found to increase with an increase in quench depth and can be characterized by the relationship of $D_{app} \sim (P - P_s)^{\nu}$ with an average value of $\nu = 2.5$.

The maximum in the scattered light intensity (I_m) and corresponding wavenumber q_m were found to show power-law behavior $q_m \sim t^{-\alpha}, I_m \sim t^{\beta}$, with time. The exponents α and β were however found to be depend on the quench depth and quench condition. Both exponents increase with quench depth while remaining a $\beta \cong 2\alpha$ relationship for all quenches, indicating that the system dimensionality may be less than 3. For the late stage of phase separation, using the apparent dimensionality $d = \beta/\alpha$, the scattered light intensity could be normalized with respect to the maximum $I_m(t)$, and the reduced scattered light intensity I_s/I_m could be scaled well with q/q_m for a given quench. However, for different quenches, the data for reduced scattered light intensity was not found to collapse to a single universal curve. The experimental data show much broader distribution in the scattered light intensity compared with the Furukawa scaling theory.

Acknowledgements

We thank K. Liu for his help with data analysis during revision of this manuscript.

References

[1] Gunton JD, Miguel MS, Sahni PS. The dynamics of first order phase transitions in phase transitions and critical phenomena, vol. 8. In: Domb C, Lebowitz JL, editors. 1983.
[2] Kiran E. Polymer formation, modification and processing in or with supercritical fluids in supercritical fluids. In: Kiran E, Levelt Sengers JMH, editors. Fundamentals for applications, Dordrecht: Kluwer Academic Publishers, 1994. p. 541–88.
[3] Van Aartsen JJ, Smolders CA. Eur Polym J 1970;6:1105.
[4] Kuwahara N, Tachikawa M, Hamano K, Kenmochi Y. Phys Rev A 1982;25:3449.
[5] Kuwahara N, Kubota K. Phys Rev A 1992;45:7385.
[6] Lal J, Bansil R. Macromolecules 1991;24:290.
[7] Tanaka H. J Chem Phys 1993;100:5323.
[8] Tanaka H. Phys Rev Lett 1993;71:3158.
[9] Xie Y, Ludwig Jr, K F, Bansil R, Gallagher PD, Konak C, Morales G. Macromolecules 1996;29:6150.
[10] Kiepen F, Borchard W. Makromol Chem 1988;189:2595.
[11] Kiepen F, Borchard W. Makromol Chem 1988;189:1543.
[12] Kiepen F, Borchard W. Macromolecules 1988;21:1784.

[13] Wells PA, de Loos ThW, Kleintjens LA. AIChE Annual Meeting, Los Angeles, Paper No. 44b, 1991.
[14] Wells PA, de Loos ThW, Kleintjens LA. Fluid Phase Equilibria 1993;106:185.
[15] Szydlowski J, van Hook WA. J Polym Sci B: Polym Phys 1991;29:1437.
[16] Szydlowski J, Rebelo L, Van Hook WA. Rev Sci Instrum 1992;63:1717.
[17] Kiran E, Zhuang W. J Supercrit Fluids 1994;7:1.
[18] Zhuang W, Kiran E. Polymer 1998;39:2903.
[19] Kiran W, Zhuang W. In: Abraham M, Sunol AK, editors. Supercritical extraction, ACS Symposium Series 670, Washington, DC: ACS, 1997. p. 2–36.
[20] Kiran E. Proceeding of the Fourth International Symposium on Supercritical Fluids, Sendai, Japan, 11–14 May 1997.
[21] Van Aartsen JJ. Eur Polym J 1970;6:919.
[22] Cahn JW, Hilliard JE. J Chem Phys 1958;28:258.
[23] Cahn JW. J Chem Phys 1959;30:1121.
[24] Cahn JW, Hilliard JE. J Chem Phys 1959;31:688.
[25] Cahn JW. Acta Metallurgica 1961;9:795.
[26] Cook HE. Acta Metallurgica 1970;18:297.
[27] Furukawa H. Adv Phys 1985;34:703.
[28] Wong N-C, Knobler CM. J Chem Phys 1978;69:725.
[29] Bailey AE, Cannell DS. Phys Rev Lett 1993;70:2110.
[30] Wenzel J, Limbach U, Schneider GM. J Phys Chem 1980;84:1991.
[31] Metz U, Schneider GM. Ber Bunsenges Phys Chem 1990;94:452.
[32] Metz U, Schneider GM. Ber Bunsenges Phys Chem 1990;94:447.
[33] Quednau J, Schneider GM. Rev Sci Instrum 1989;60:3685.
[34] Sieber M, Woermann D. Ber Bunsenges Phys Chem 1991;95:15.
[35] Wells PA, de Loos ThW, Kleintjens LA. Fluid Phase Equilibria 1995;106:185.
[36] Derham KW, Goldsbrough J, Gordon M. Pure Appl Chem 1974;38:97.
[37] Debye P. J Chem Phys 1959;31:680.
[38] Debye P, Woermann D, Chu B. J Chem Phys 1962;80:851.
[39] Debye P, Woermann D. J Chem Phys 1960;31:1746.
[40] Kojima J, Nakayama Y, Takenaka M, Hashimoto T. Rev Sci Instrum 1995;66:4066.
[41] Xiong Y, Kiran E. Rev Sci Instrum 1998;69:1463.
[42] Binder K, Stauffer D. Phys Rev Lett 1974;33:1006.
[43] Hosokawa H, Nakata M, Dobashi T. J Chem Phys 1993;98:10 078.
[44] Dobashi T, Nakata M, Kaneko MJ. J Chem Phys 1980;72:6685.
[45] Shen W, Smith GR, Knobler CM, Scott RL. J Phys Chem 1991;95:3376.
[46] Imre A, van Hook WA. J Poly Sci B: Polym Phys 1996; 34:751.
[47] Koningsveld R, Kleintjens LA. Macromolecules 1971;4:637.
[48] Yeo S, Kiran E. J Supercrit Fluids 1999;15:261.
[49] Lin CC, Jeon HS, Balsara NP, Hammouda B. J Chem Phys 1995;103:1957.
[50] Xiong Y. PhD Dissertation, Kinetics of pressure-induced phase separation in polymer solutions: a time- and angle-resolved light scattering study, University of Maine, 1998.
[51] Stanley HE. Introduction to phase transition and critical phenomena, Oxford: Oxford University Press, 1971.
[52] Siggia ED. Phys Rev A 1979;20:595.
[53] Hashimoto T. Phase Transitions 1988;12:47.
[54] Liu K, Kiran E. J Supercrit Fluids 1999;16.
[55] Porod G. In: Glatter O, Kratky O, editors. Small angle X-ray scattering, New York: Academic Press, 1982 p. 30.